ISOMAse
International Society of Ocean, Mechanical and Aerospace Scientists and Engineers
Journal of Ocean, Mechanical and Aerospace
-Science and Engineering-
30th March 2025. Vol.69 No.1
March 30, 2025

Advanced Design and Simulation of Spreader Bar for Safe Lifting of 80 Tons Pressure Vessel by Using Finite Element Analysis

Bagus Kusuma[a], Fardin Hasibuan[a*], Arif Rahman Hakim[a] and Eka Chandra Yulianta[b]

[a)]*Program Studi Teknik Mesin, Fakultas Teknik, Universitas Riau Kepulauan, Batam, 29422, Indonesia*
[b)]*Project Manager, PT. NOV profab, Batam, 29444, Indonesia*

*Corresponding author: fardin.hasibuan123456@gmail.com

Paper History

Received: 07-January-2025
Received in revised form: 27-February 2025
Accepted: 30-March-2025

ABSTRACT

This study focuses on designing and optimizing a spreader bar for lifting a pressure vessel are 14,214 millimeters in length, 4,364 millimeters in diameter, and a total weight of 80 tons, addressing challenges in load distribution and safety. The spreader bar, constructed from API 5L X52material, was modeled using SolidWorks and analyzed through Finite Element Analysis (FEA) under four lifting configurations. Key parameters such as stress, strain, and displacement were evaluated to ensure compliance with safety standards. Results indicated that all configurations meet the required safety factor of 1.5, with simulation 3 (C-C) demonstrating the best performance in minimizing stress and displacement. The discussion highlights the design's ability to balance structural integrity, material efficiency, and operational safety. The study concluded that the proposed spreader bar design enhances workplace safety, reduces the risk of equipment failure, and provides a cost-effective solution for heavy lifting tasks.

KEYWORDS: *Finite element analysis, Heavy lifting, Pressure vessel, Safety factor, Spreader bar.*

1.0 INTRODUCTION

Lifting heavy loads is a significant activity in various industrial sectors, such as construction, manufacturing, and logistics [1]. Cranes are the leading equipment used in material handling because they can perform the task safely and efficiently [2]. A pressure vessel is one of the materials to be lifted using a crane. One of the key considerations during the lifting process is ensuring the equipment remains safe and free from defects. Several issues are often encountered during the lifting process, such as excessive tension on the equipment and friction between the sling and the lifted equipment.

Furthermore, a spreader bar is needed as a supporting tool to reduce tension or avoid overstressing certain parts of the equipment during the lifting process.However, additional equipment like a spreader bar becomes crucial when lifting large, long, or uneven loads [3]. The spreader bar distributes the lifting force evenly, aiming to prevent deformation or damage to the load and maintain stability during the lifting process [3-4].

The concept of the safety factor is used throughout the mechanics and design sequence in mechanical engineering. In its simplest form, it is presented as the ratio of the failure strength of a mechanical component to the expected stress that the part will see in service, safety factor is equal tostrength divided by stress [5-8]. The design criteria are acceptable when they meet the safety criteria mentioned above, where the material strength is greater than the stress acting on the components of the designed equipment.

The design of the spreader bar requires special attention to several technical factors to ensure its optimal function [9]. First, the characteristics of the load must be considered [10]. The load to be lifted can have varying shapes, sizes, and mass distributions. This makes adjusting each spreader bar design necessary according to the load being lifted [3]. The crane's capacity is also a key factor that must be considered so that the spreader bar can support the lifting weight without damage. The length of the spreader bar must also match the length of the load to be lifted to maintain stability during the lifting process [9].

Furthermore, the material used to construct the spreader bar must be carefully selected. The correct material choice will affect the spreader bar's strength, durability, and weight. Additionally, connecting the spreader bar to the lifting rope or sling must be done correctly to ensure the lifting process is safe and efficient. If the spreader bar is not designed correctly, it could increase the risk of workplace accidents and damage to the lifted material. The top priorities are manufacturing costs, materials, crane usage, and worker safety. The existing structure in the lifting process must not be damaged or overstressed [11]. Therefore, every stage of the spreader bar design must be based on a thorough analysis to ensure optimal safety and operational efficiency [12].

Previous studies have explored various designs and materials for spreader bars. At the same time, their weight and fabrication complexity limit robust, Conventional solid beam

designs. Alternative materials, such as aluminum and composite materials, have been investigated for lightweight applications. However, their use in heavy lifting is constrained by cost and availability. This study builds upon these findings by introducing a pipe-based design that balances strength, weight, and price.

One of the key innovations introduced in this study is using a computer simulation method based on finite element analysis (FEA) [13]. This method can more accurately model the stress and deformation distribution occurring in the spreader bar and load during the lifting process. This simulation will provide deeper insights into the spreader bar's performance in real-world situations, allowing the design to be more precise and tailored to field requirements.

This study aims to design a spreader bar capable of lifting a pressure vessel with14214 millimeters in length, 80tons. The primary focus of this design is to create a structure that can evenly distribute the lifting force to lift and move the pressure vessel. Doing so is expected to minimize the potential for excessive stress on the load and enhance safety during the lifting process. The novelty of this research lies in developing a spreader bar design that optimizes load distribution and accounts for loads with more complex characteristics. This study contributes to improving workplace safety in the industrial sector.

Work accidents related to lifting equipment failure often occur when heavy loads are lifted with uneven force distribution. An optimized spreader bar design can minimize the risk of equipment failure. This improves crane operator safety, reduces equipment maintenance costs, and prevents damage to the lifted materials.

2.0 METHOD

2.1 Material

The spreader bar is designed to lift a pressure vessel weighing 80 tons, as shown in Figure 1. Pipes are typically used in the manufacturing of spreader bars due to their strength and durability. For the creation of pad eyes, plates are the preferred material, providing the necessary support. The dimensions of the spreader bar are shown in Figure 2, offering a detailed representation of its size and structure. Figure 3 illustrates the dimensions of the pressure vessel, highlighting its specifications. The specifications of the materials are shown in Table 1.

2.2 Design

The spreader bar is designed according to the vessel's dimensions to be lifted. The distance between the lifting lugs has already been determined to provide uniform lifting points on the vessel. The first step in designing a spreader bar for lifting a pressure vessel, which is used as a heat exchanger, involves considering the material properties of the vessel. The shell of the pressure vessel is made of medium carbon steel, while the tubes, which number 5200, are made of stainless steel. The overall dimensions of the pressure vessel are 14214 millimeters in length, 4364 millimeters in diameter, and a total weight of 80 tons. The design process begins by creating 3D models of both the spreader bar and the pressure vessel using SolidWorks. This design phase ensures that both components are accurately represented with their respective shapes and dimensions. The material properties of the vessel are also defined in the software to simulate realistic behavior during the lifting process.

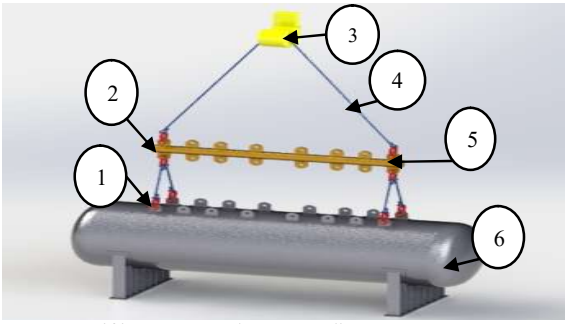

1. Lifting Lug Vessel
2. Spreader Bar
3. Hook
4. Sling
5. Lifting Lug Spreader Bar
6. Pressure Vessel

Figure 1: Component design

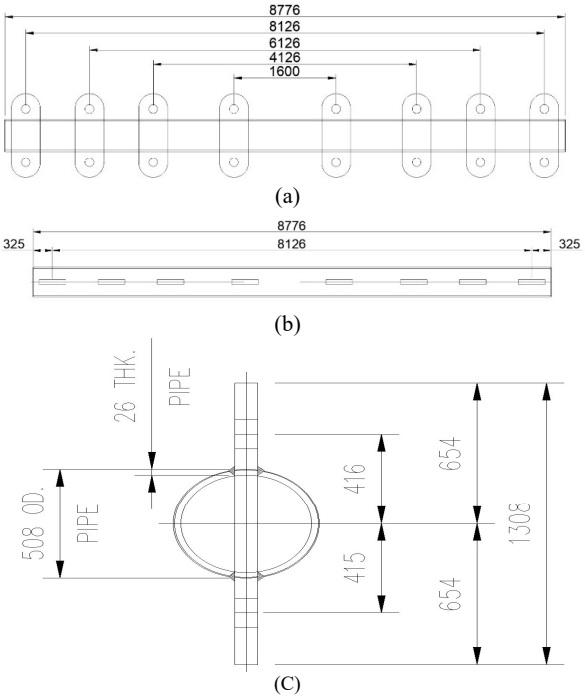

Figure 2: Dimension: (a) distance of lifting lug, (b) length of spreader bar, and (c) diameter of spreader bar

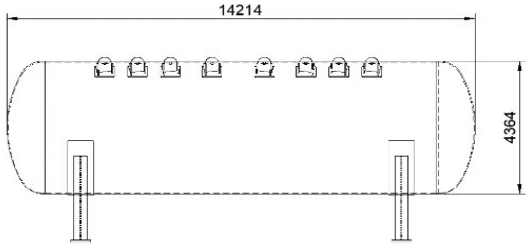

Figure 3: Dimension of pressure vessel

Table 1: Material properties of component design [14-16]

	Components				
	Lifting Lug	Pressure Vessel	Spreader Bar	Sling	Hook
Material	S355 J2	SA516 Gr 70	API 5L X52	Webbing polyester	S355 J2
Yield strength	0.355GPa	0.260 to 0.450GPa	0.360GPa	0.010 to 0.700GPa	0.355GPa
Tensile strength	0.51to 0.68GPa	0.485 to 0.620GPa	0.450GPa	0.020 to1GPa	0.510 to 0.680GPa
Elastic Modulus	190 to 210GPa	200GPa	210GPa	2.7GPato 3.5GPa	200.000GPa

2.3 Simulation

This design calculation used the SolidWorks application. SolidWorks is a solid modeling software used to produce parts and assembly drawings by utilizing parametric features. Here, parameters refer to constraints. Its values determine the shape or geometry of the model[17]. The step-by-step instructions are as follows: creating a study, assigning material, applying fixtures, applying loads, meshing the assembly, running the analysis, and visualizing the results.

The lifting points on the spreader bar were modeled in four different condition simulations: simulation 1: A-A, simulation 2: B-B, simulation 3: C-C, and simulation 4: D-D.

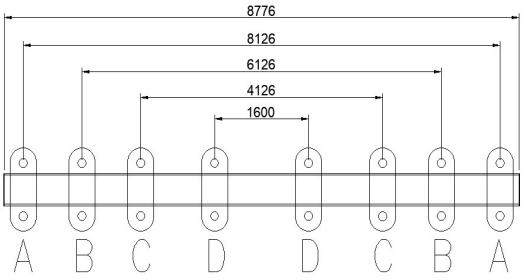

Figure 4: Lifting lug position for condition simulation

After performing these simulations, the results obtained:

1. The distribution of stress, strain, and displacement at each condition,
2. Axial force, shear force, torque, bending moment at sling
3. Reaction force, reaction moment at hook.

2.4 Position Simulation

All condition simulations will be simulated to determine the loading conditions that occur.In SolidWorks, components can be designed as part of a 3D model that includes interconnected components, where movement or load transfer can be analyzed and simulated. Several positions that were simulated are connected to each other to transmit motion or force. A mechanism involving multiple components, such as the hook, spreader bar, and pressure vessel, was used to describe this system [18].

The simulation was conducted at specific components, shown in Figure 5 to analyze the behavior of the tested system or object. These components were carefully selected from critical areas to ensure a more precise assessment of the system's response under given conditions. By focusing on these key locations, this approach allows for a detailed performance evaluation and helps identify potential issues that may require improvement. The selected points are illustrated in Figure 5.

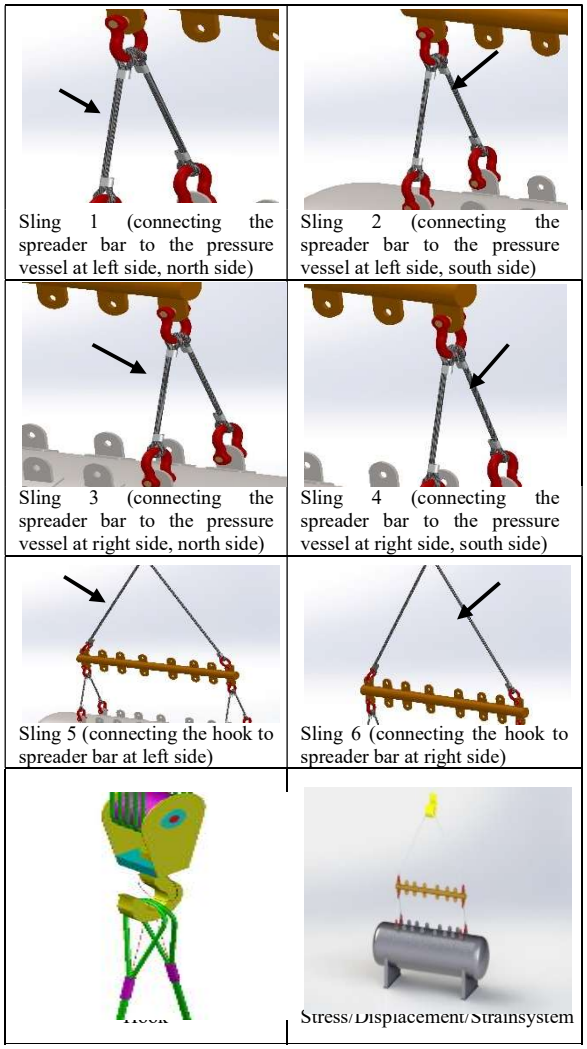

Figure 5: Position of simulation

2.5 Simulation Setup

FEA is a numerical approach used to evaluate engineering designs thoroughly. The process begins with creating a geometric representation of the design. Subsequently, the model is divided into several small, simple parts called elements, which are interconnected through points known as nodes. This division stage, meshing, transforms the model into a network of connected elements. Meshing plays a crucial role in the design analysis process. FEA software automatically

generates a mesh combination of solid, shell, and beam elements. Solid elements are used for complex 3D structures, shell elements for thin components like metal plates, and beam elements for specific structural parts [19].

Table 2: Study properties of simulation

Mesh type	Solid Mesh
Mesher Used	Blended curvature-based mesh
Total Nodes	76780
Total Elements	38366
Maximum Aspect Ratio	52.708
% of elements with Aspect Ratio < 3	3.74
Percentage of elements with Aspect Ratio > 10	2.16
Total Nodes	76780
Total Elements	38366
Maximum Aspect Ratio	52.708

3.0 RESULT

3.1 Simulation 1 (A-A)

The lifting position of the pressure vessel is carried out by placing the sling on the lifting lug as shown in Figure 6. The result of the FEA for simulation 1(A-A) can be seen in Tables 3, 4 and 5, as well as Figure 7.

Table 3: Resultant of loads at sling

	Location		
Component	Sling 1	Sling 2	Sling 3
Axial Force (kN)	172.58	172.84	172.39
Component	Sling 4	Sling 5	Sling 6
Axial Force (kN)	172.97	411.06	410.99

Table 4: Resultant of loads at hook

Component	Hook
Reaction force (kN)	558.13
Reaction Moment (N.m)	0

Table 5: Result of simulation 1(A-A)

	Stress	
	Maximum	Minimum
Value	69.11 MPa	1.62 e-09 MPa
Location	Node: 73469	Node: 69423
	Displacement	
	Maximum	Minimum
Value	101 mm	0 mm
Location	Node: 436	Node: 69226
	Strain	
	Maximum	Minimum
Value	2.09 e-04	3.38 e-08
Location	Element: 34756	Element: 19713

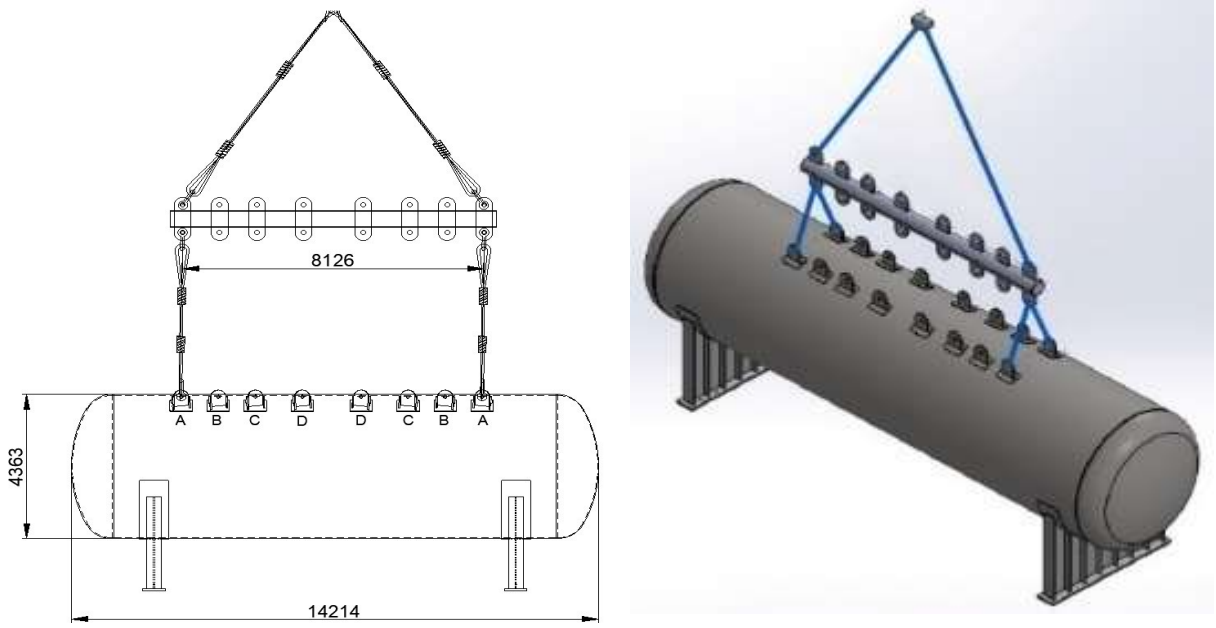

(a) (b)

Figure 6: (a) Position design of 2D, (b) Position design of 3D

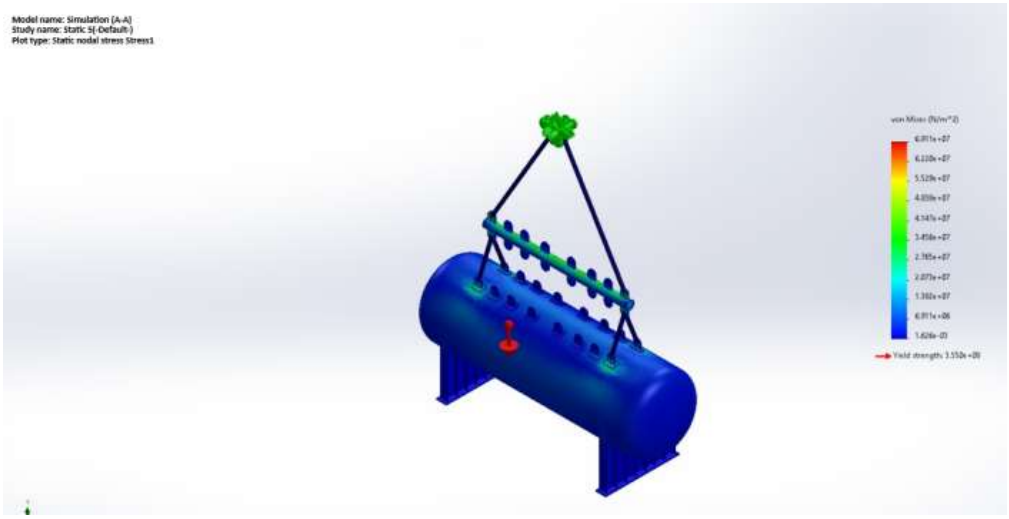

(a)

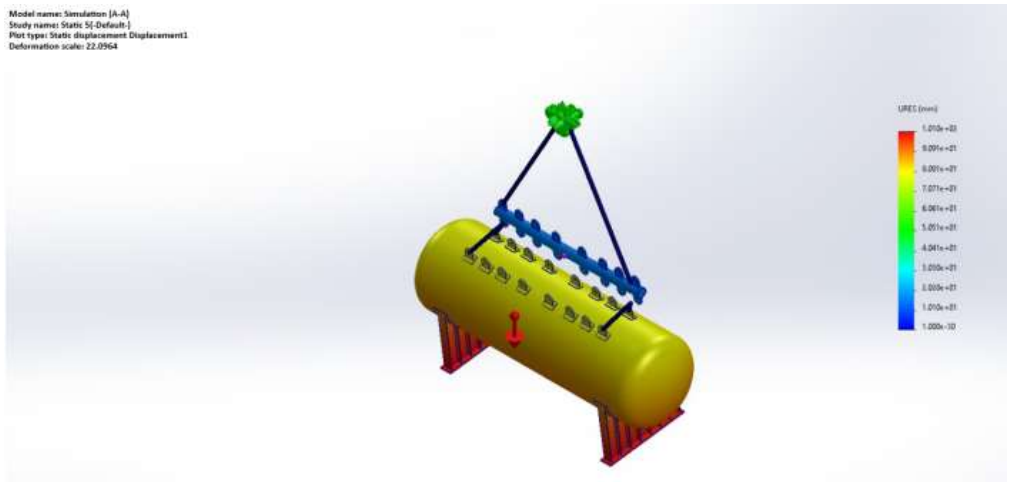

(b)

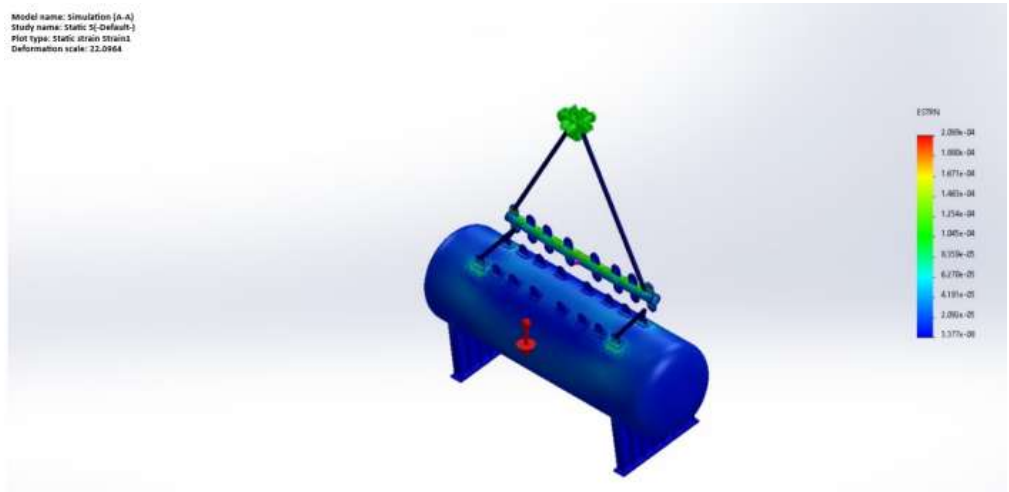

(c)

Figure 7: Distribution: (a) Stress, (b) Displacement, and (c) Strain

3.2 Simulation 2 (B-B)

The lifting position of the pressure vessel is achieved by placing the sling on the lifting lug, as depicted in Figure 8. This method ensures proper alignment and secure lifting during the operation. The results of the FEA for simulation 2 are presented in Tables 6, 7, and 8, along with Figure 9. These tables and figure provide detailed insights into the simulation's outcomes.

Table 6: Resultant of loads at sling

	Location		
Component	Sling 1	Sling 2	Sling 3
Axial Force (kN)	173.56	173.72	172.81
Component	Sling 4	Sling 5	Sling 6
Axial Force (kN)	173.61	386.76	386.65

Table 7: Resultant of loads at hook

Component	Hook
Reaction force (kN)	558.04
Reaction Moment(N.m)	0

Table 8: Result of simulation 2 (B-B)

	Stress	
	Maximum	Minimum
Value	63.93 MPa	1.86 e-09 MPa
Location	Node: 74300	Node: 69423
	Displacement	
	Maximum	Minimum
Value	69.01mm	0 mm
Location	Node: 668	Node: 69226
	Strain	
	Maximum	Minimum
Value	1.98e-04	1.44e-08
Location	Element: 5825	Element: 35825

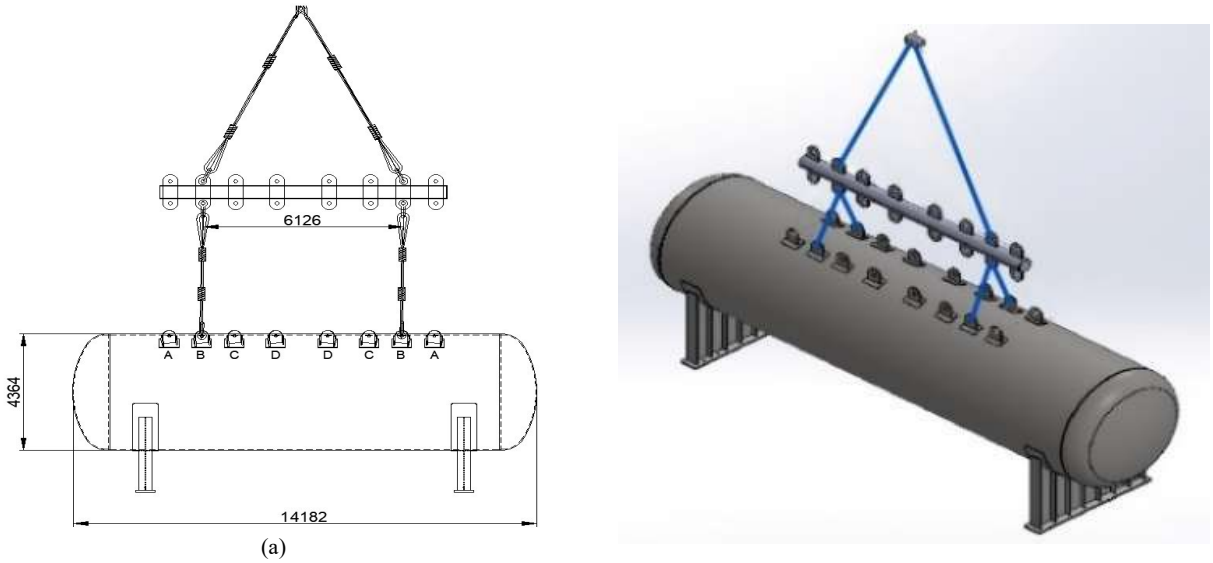

(a)

Figure 8: Position design 2D, (b) Position design 3D

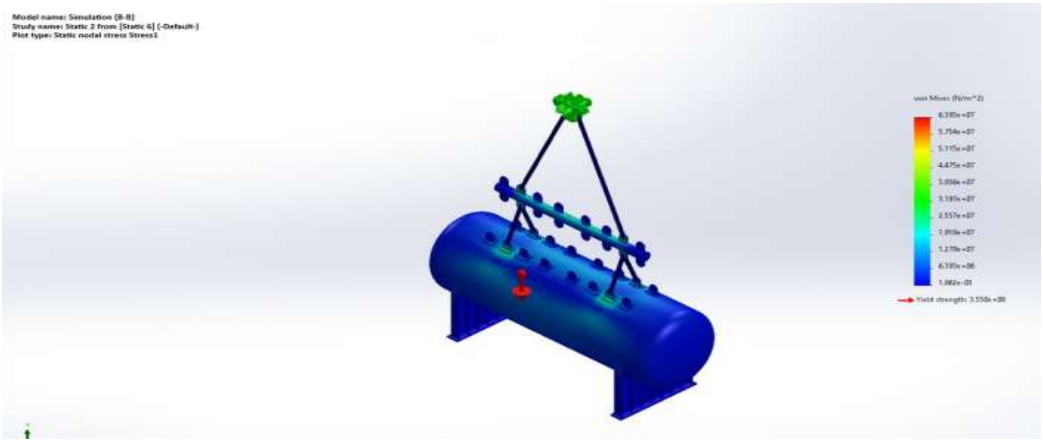

(a)

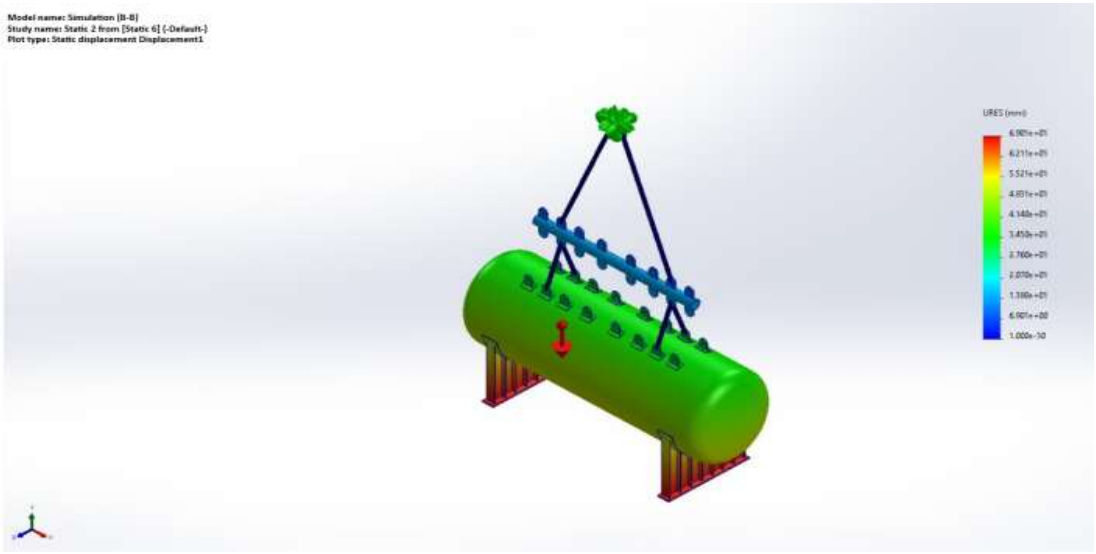

(b)

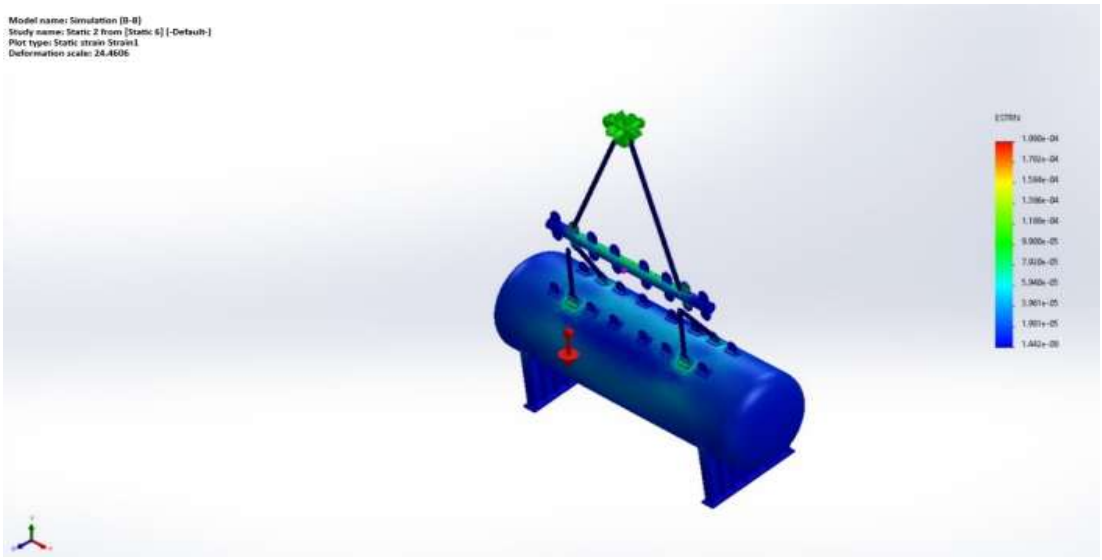

(c)

Figure 9: Distribution of: (a) Stress, (b) Displacement, and (c) Strain

3.3 Simulation 3 (C-C)

The lifting position of the pressure vessel is done by placing the sling on the lifting lug as shown in Figure 10. The result of the FEA for simulation 3 can be seen in Tables 9, 10, and 11, as well as Figure 11.

Table 10: Resultant of loads at hook

Component	Hook
Reaction force (N)	557.97
Reaction Moment(N.m)	0

Table 9: Resultant of loads at sling

	Location		
Component	Sling 1	Sling2	Sling3
Axial Force (kN)	173.45	173.89	173.37
Component	Sling 4	Sling 5	Sling 6
Axial Force (kN)	173.85	368.59	368.42

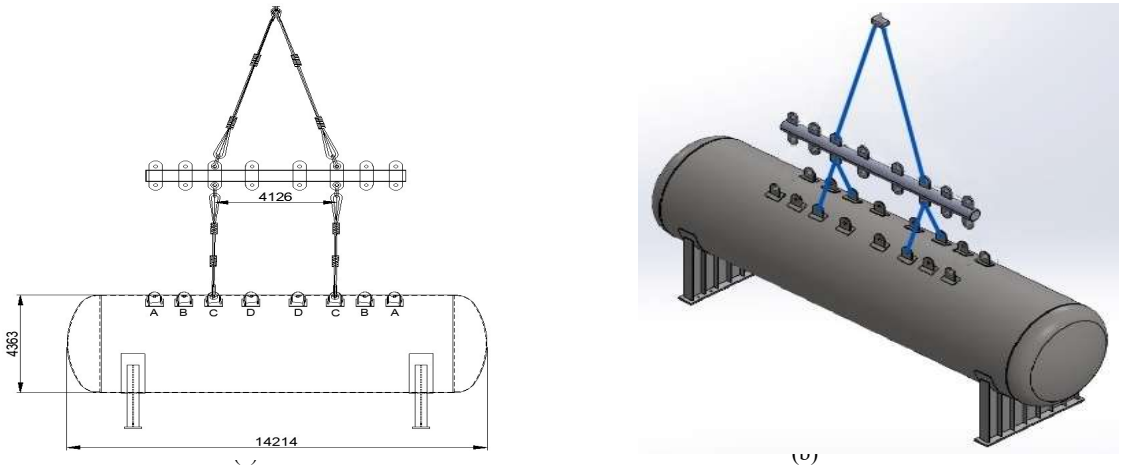

Figure 10: (a) Position design 2D, (b) Position design 3D

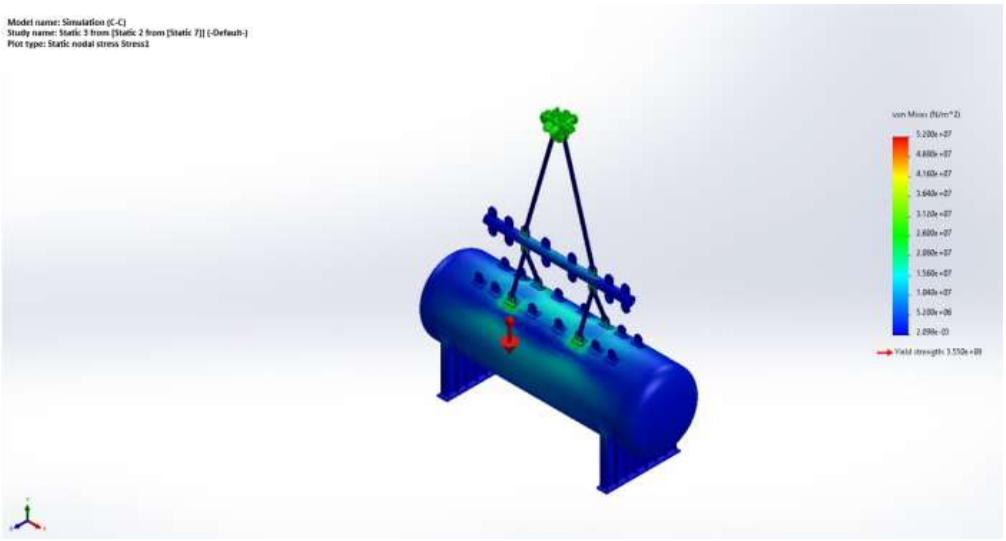

(a)

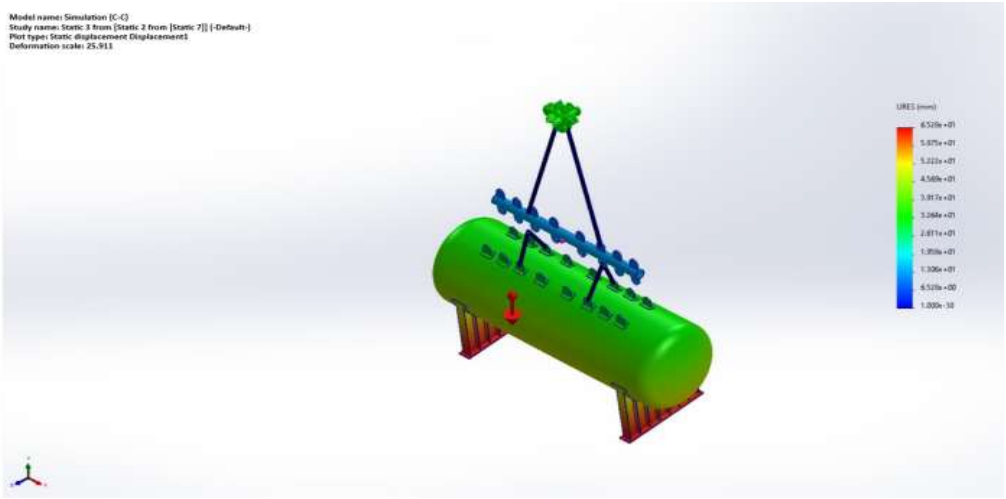

(b)

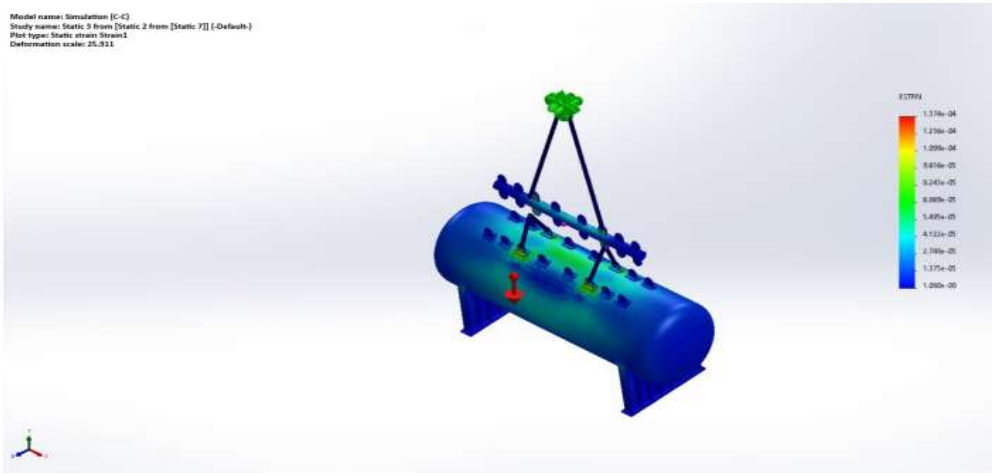

(c)

Figure 11: Distribution of: (a) Stress, (b) Displacement, and (c) Strain

Table 11: Result of simulation 3 (C-C)

	Stress	
	Maximum	Minimum
Value	52.0 MPa	2.098 e-09 MPa
Location	Node: 70209	Node: 69423
	Displacement	
	Maximum	Minimum
Value	65.28mm	0mm
Location	Node: 436	Node: 69226
	Strain	
	Maximum	Minimum
Value	1.37e-04	1.08e-08
Location	Element: 36798	Element: 37631

3.4 Simulation 4 (D-D)

The lifting position of the pressure vessel is carried out by placing the sling on the lifting lug as shown in Figure 12. The result of the FEA for simulation 2 can be seen in Tables 12, 13, and 14, as well as Figure 13.

Table 12: Resultant of loads at Sling

	Location		
Component	Sling1	Sling2	Sling3
Axial Force (kN)	173.61	174.31	173.69
Component	Sling 4	Sling 5	Sling 6
Axial Force (kN)	173.86	355.93	355.48

Table 13: Resultant of loads at hook

Component	Hook
Reaction force (N)	557.92
Reaction Moment(N.m)	0

4.0 DISCUSSION

Based on the results of the simulation at Section 3, it can be concluded that the points experiencing the highest loading conditions are as shown in Table 15.

Table 14: Result of simulation 4 (D-D)

	Stress	
	Maximum	Minimum
Value	53.4 MPa	2.39e-09 MPa
Location	Node: 69562	Node: 69423
	Displacement	
	Maximum	Minimum
Value	69.05 mm	0 mm
Location	Node: 668	Node: 69226
	Strain	
	Maximum	Minimum
Value	1.34e-04	1.15e-08
Location	Element: 37178	Element: 35863

Table 15: Result of simulation

	Simulation 1 (A-A)	Simulation 2 (B-B)	Simulation 3 (C-C)	Simulation 4 (D-D)
Sling Axial Force (kN)	Sling 5 411.06	Sling5 386.7	Sling 5 368.59	Sling 5 355.93
Hook Reaction Force (kN)	558.13	558.04	557.97	557.92
Stress Maximum (MPa)	69.11	63.93	52.0	53.4
Displacement Maximum (mm)	101	69.01	65.28	69.05
Strain Maximum	2.09 e-04	1.98e-04	1.37e-04	1.34e-04

4.1 Simulation1 (A-A)

Sling

The highest axial force occurs in sling 5 with a value of 411.06kN. The sling is made of 60 tons webbing sling material, which has a load-bearing capacity of 588.6kN. The load-bearing capacity of the webbing sling material is greater than the force acting on the sling, so the material used is safe.

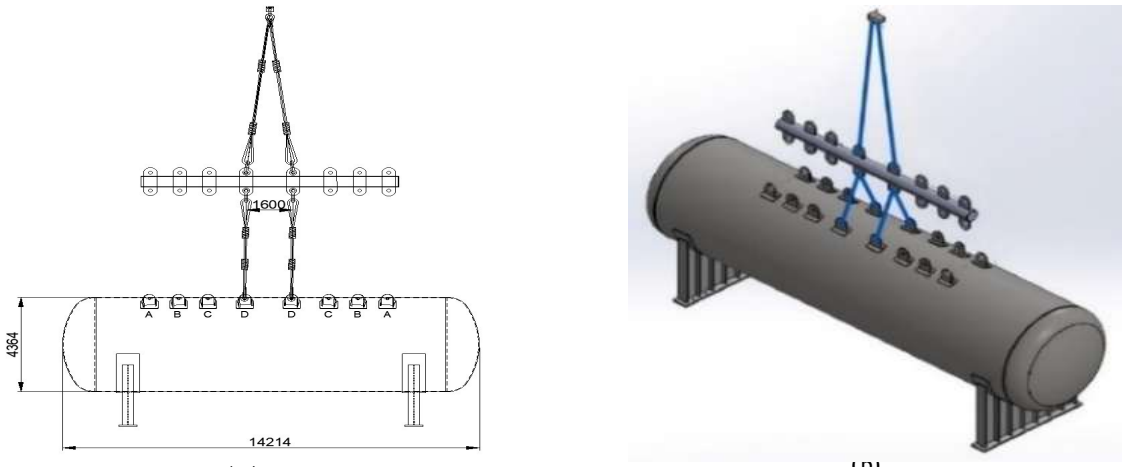

(a) (b)

Figure 12: (a) Position design of 2D, (b) Position design of 3D

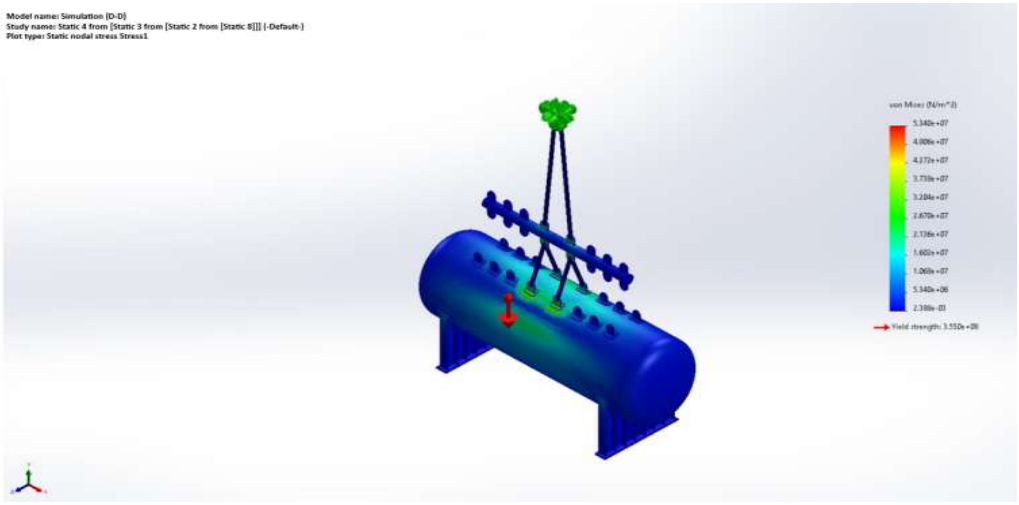

(a)

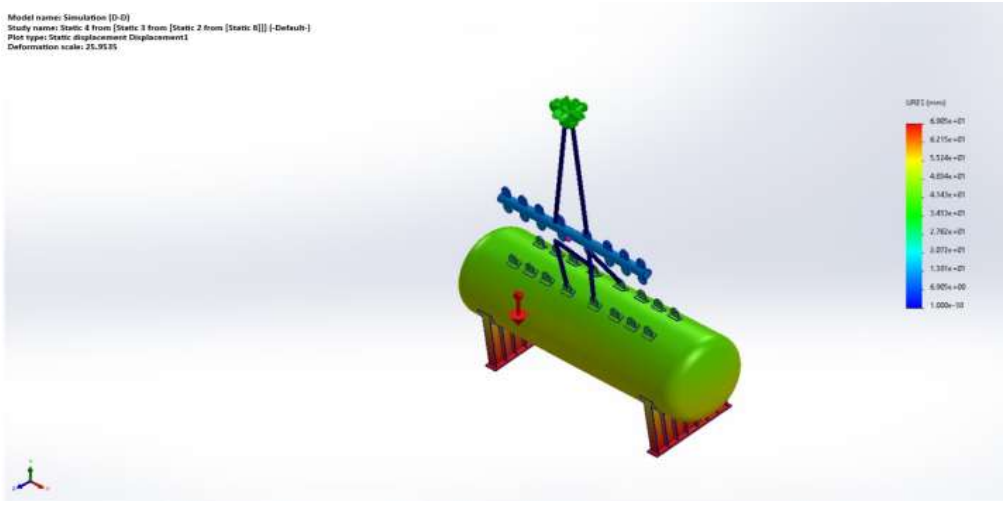

(b)

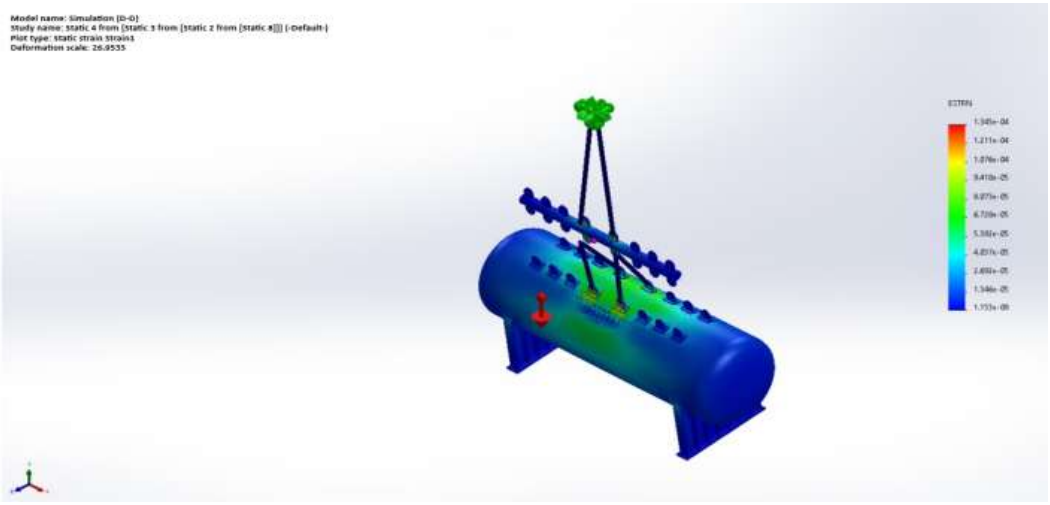

(c)

Figure 13: Distribution of: (a) Stress, (b) Displacement, and (c) Strain

Hook

The reaction force acting on the hook is 558.13kN, and the hook's capacity to withstand the load is 3330kN. Therefore, the hook material is capable of withstanding the load.

Stress and Displacement Distribution

The maximum stress acting on the spreader bar is 69.11 MPa, and the material strength is 355 MPa. Therefore, the stress acting on the spreader bar is lower than the material strength, indicating that the material used is safe. The maximum displacement acting on the pressure vessel is 101 mm, and the length of the pressure vessel material is 14214mm. The maximum deflection required is 1% of the length, which is 142.14 mm. Thus, the deflection that occurs is smaller than the maximum deflection required, meaning the lifting process is still in a safe condition.

4.2 Simulation 2(B-B)

Sling

The highest axial force occurs in Sling 5 with a value of 386.7kN. The sling is made of 60 tons webbing sling material, which has the capability to withstand a load of 588.6kN. The load-bearing capacity of the webbing sling material is greater than the force acting on the sling, so the material used is safe.

Hook

The reaction force acting on the hook is 558.04kN, and the hook's capacity to withstand the load is 3330kN. Therefore, the hook material is capable of withstanding the load.

Stress and Displacement Distribution

The maximum stress acting on the spreader bar is 63.9 MPa, and the material strength is 355 MPa. Therefore, the stress acting on the spreader bar is smaller than the material strength, indicating that the material used is safe. The maximum displacement acting on the pressure vessel is 69.01 mm, and the length of the pressure vessel is 14214 mm. The maximum deflection required is 1% of the length, which is 142.14 mm. Therefore, the displacement that occurs is smaller than the maximum required deflection, meaning the lifting process is still in a safe condition.

4.3 Simulation3 (C-C)

Sling

The highest axial force occurs in Sling 5 with a value of 368.59kN. The Sling is made of 60tons webbing sling material, which has a load-bearing capacity of 588.6kN. The load-bearing capacity of the webbing sling material is greater than the force acting on the sling, so the material used is safe.

Hook

The reaction force acting on the hook is 557.97kN, and the hook's capacity to withstand the load is 3330kN. Therefore, the hook material is capable of withstanding the load.

Stress and Displacement Distribution

The maximum stress acting on the spreader bar is 52.0 MPa, and the material strength is 355 MPa. Therefore, the stress acting on the spreader bar is smaller than the material strength, indicating that the material used is safe. The maximum displacement acting on the pressure vessel is 65.28 mm, and the length of the pressure vessel material is 14214 mm. The maximum deflection required is 1% of the length, which is 142.14 mm. Thus, the displacement that occurs is smaller than the maximum required deflection, meaning the lifting process is still in a safe condition.

4.4 Simulation4 (D-D)

Sling

The highest axial force occurs in Sling 5 with a value of 355.93kN. The sling is made of 60 tons webbing sling material, which has a load-bearing capacity of 588.6kN. The load-bearing capacity of the webbing sling material is greater than the force acting on the sling, so the material used is safe.

Hook

The reaction force acting on the hook is 557.97kN, and the hook's capacity to withstand the load is 3330kN. Therefore,

the hook material is capable of withstanding the load.

Stress and Displacement Distribution

The maximum stress acting on the spreader bar is 53.4 MPa, and the material strength is 355 MPa. Therefore, the stress acting on the spreader bar is smaller than the material strength, indicating that the material used is safe. The maximum displacement acting on the pressure vessel is 69.05 mm, and the length of the pressure vessel is 14214 mm. The maximum deflection required is 1% of the length, which is 142.14 mm. Thus, the displacement that occurs is smaller than the maximum required deflection, meaning the lifting process is still in a safe condition.

Therefore, based on those results of the simulation analysis above, it can be concluded that all the results of the simulation are in a safe condition.

Table 16: Result of condition simulation

Component	Simulation			
	1 (A-A)	2 (B-B)	3 (C-C)	4 (D-D)
Lifting Lug Vessel	Safe	Safe	Safe	Safe
Spreader Bar	Safe	Safe	Safe	Safe
Hook	Safe	Safe	Safe	Safe
Sling	Safe	Safe	Safe	Safe
Lifting Lug Spreader Bar	Safe	Safe	Safe	Safe

The locations for lifting the pressure vessel are safe at all positions. However, based on the smallest stress and displacement that occur, the highest safety factor is found in simulation 3 (C-C), followed by simulation 4 (D-D), simulation 2 (B-B), and finally simulation 1 (A-A).

5. CONCLUSION

Based on the results of the simulation for the design of a pipe-shaped spreader bar with a pipe length of 8,776 mm and a diameter of 508 mm, made of API 5L X52 material, to lift a pressure vessel with a length of 14,214 mm and a diameter of 4,364 mm made of SA 516 Gr.70 material, along with polyester webbing slings and a hook made of S355 J2 material, the system is capable of lifting a pressure vessel with a weight of 80 tons. With a simulation safety factor of 1.5 based on the von Mises criteria, all simulation conditions are safe, and the safest configuration is simulation 3 (C-C).

REFERENCES

[1] Purwono, R., Supomo, H. & Suastika, I.K. (2018). Technical and economic analysis of the development of steel bridge on ship industry for diversified business. *Semantics Scholar*. Available at https://api.semanticscholar.org/CorpusID:211794650.

[2] Herrera-Pérez, V., Salguero-Caparrós, F., Pardo-Ferreira, M. del C. & Rubio-Romero, J.C. (2023). Key factors in crane-related occupational accidents in the Spanish construction industry (2012–2021). *International Journal of Environmental Research and Public Health, 20*(22), 7080. https://doi.org/10.3390/ijerph20227080.

[3] Ashariyani, I.D.A., Sidi, P. & Nugroho, P.N.A. (2023). Perancangan spreader bar sebagai alat bantu pengangkatan pada proses erection. In *Proceedings Conference On Design Manufacture Engineering And Its Application*, 7(1).

[4] Wandono, F.A., Nuranto, A.R., Nurrohmad, A., Hafid, M. & Bintoro, A. (2023). Design improvement of the amphibious aircraft spreader bar using a composite structure. *Machine Learning and Information Processing: Proceedings of ICMLIP 2023*. Available at https://api.semanticscholar.org/CorpusID:266254325.

[5] Childs, P.R.N. (2013). *Mechanical design engineering handbook*. https://doi.org/10.1016/C2011-0-04529-5.

[6] He, F. (2012). Research on accuracy design of mechanical design. *Applied Mechanics and Materials, 184–185*, 412–416. https://doi.org/10.4028/www.scientific.net/AMM.184-185.412.

[7] Musto, J.C. (2010). The safety factor: case studies in engineering judgment. *International Journal of Mechanical Engineering Education*, *38*(4), 286-296.

[8] Sreeram, T.R. & Katti, V.A. (2007). A multi-criteria decision making model for the design of machine structures. *SAE Technical Papers*. https://doi.org/10.4271/2007-01-1479.

[9] Ramadhan, M., Saputra, I. & Baharudin, B. (2022). Stress dan displacement pada spreader beam akibat variasi pembebananan. *Jurnal Teknik dan Rekayasa, 10*(1). Available at http://jurnal.polibatam.ac.id/index.php/JATRA.

[10] Zakaria, C.Z. & Aziz, N.A. (2018). Finite element analysis of spreader bar by utilizing the arrangement and connection of padeyes. *Journal of Mechanical Engineering and Technology (JMET)*, *10*(2), 77-97.

[11] Imad, H.M. & Primaningtyas, W.E. (2023). Construction design of lifting spreader for lifting harp evaporator using finite element method. *JISO: Journal of Industrial and Systems Optimization*, *6*(2), 124-130.

[12] Mustapa, M.A., Rosli, N.N. & Rozali, R.H. (2024). An investigation of lifting cranes for loading and offloading at offshore terminals. *Advanced Structured Materials, 208*, 387–405. https://doi.org/10.1007/978-3-031-56844-2_34.

[13] Dragne, C., Radu, C. & Iliescu, M. (2022). Mechanical engineering of robotic systems by SolidWorks. *International Journal of Modern Manufacturing Technologies, 14*(2), 61–68. https://doi.org/10.54684/ijmmt.2022.14.2.61.

[14] Massa, D. J. (2023). Polyester materials and properties. *Polyester Films: Materials, Processes and Applications*, 19-46.

[15] Moss, D.R. (2004). Pressure Vessel Design Manual. Elsevier.

[16] Steel-S355-Technical-Details. https://www.meadinfo.org/2015/08/s355-steel-properties.html.

[17] Mariappan, S.M. & Veerabathiran, A. (2016). Modelling and simulation of multi spindle drilling redundant SCARA robot using Solid Works and MATLAB/SimMechanics. *Revista Facultad de Ingeniería, 81*, 63–72. https://doi.org/10.17533/udea.redin.n81a06.

[18] Ranjbarkohan, M., Rasekh, M., Hoseini, A.H., Kheiralipour, K. & Asadi, M.R. (2011). Kinematics and kinetic analysis of the slider-crank mechanism in Otto linear four-cylinder Z24 engine. *Journal of Mechanical Engineering Research*, 3(10). Available at http://www.academicjournals.org/jmer.

[19] Topare, N.S., Raut, S.J. & Attar, S.J. (2012). 3D model design and simulation of photo catalytic reactor for degradation of dyes using Solid Works software. *Sadguru Publications*. Available at www.sadgurupublications.com.

JOMAse | Received: 07-January-2025 | Accepted: 30-March-2025 | [(69) 1: 18-30]
Published by International Society of Ocean, Mechanical and Aerospace Scientists and Engineers, www.isomase.org., ISSN: 2354-7065 & e-ISSN: 2527-6085